

Electronic Supplementary Information:

Solution-Phase Synthesis and Thermal Conductivity of Nanostructured CdSe, In₂Se₃, and Composites Thereof

Yuanyu Ma,^a Minglu Liu,^b Abbas Jaber,^b and Robert Wang^{a,b}

^aMaterials Science & Engineering, Arizona State University

^bMechanical Engineering, Arizona State University

Contents

I. Nanocomposite Synthesis

- I.1. Materials
- I.2. CdSe Nanocrystal Synthesis
- I.3. (N₂H₄)₂(N₂H₅)₂In₂Se₄ Precursor Synthesis
- I.4. Ligand Exchange Process
- I.5. Nanocomposite Formation

II. Materials Characterization

- II.1. Thermogravimetric Analysis
- II.2. Transmission Electron Microscopy
- II.3. Scanning Electron Microscopy
- II.4. Elemental Composition Characterization
- II.5. X-ray Diffraction

III. Calculation of Relative Peak Intensities for CdSe and CdIn₂Se₄

IV. Cahill-Pohl Model Calculation

Figures

- Figure S1. X-ray diffraction of nanocomposite powders
- Figure S2. Energy-dispersive x-ray spectroscopy with nanoscale resolution on composite
- Figure S3. Energy-dispersive x-ray spectroscopy with microscale resolution on composite
- Figure S4. Thermal conductivity of nanocomposite films with varying thicknesses
- Figure S5. Ratio of profilometer film thickness to Rutherford backscattering spectroscopy film thickness for composites with varying In₂:Cd ratio.
- Figure S6. Ratio of profilometer film thickness to Rutherford backscattering spectroscopy film thickness for composites with varying profilometer film thickness.

I. Nanocomposite Synthesis

I.1. Materials:

CdCO₃ (99.998%), stearic acid (90%+) and selenium shot (99.999%) were purchased from Alfa Aesar. Trioctylphosphine (97%) and trioctylphosphine oxide (99%) were purchased from Strem Chemicals. Hydrazine (anhydrous, 98%) was purchased from Sigma Aldrich and then further purified via distillation prior to use.

I.2. CdSe Nanocrystal Synthesis

Wurtzite phase CdSe nanocrystals were synthesized by the hot injection method reported by Qu *et al.*¹ In a typical CdSe nanocrystal synthesis, 0.069 g CdCO₃ and 4 g stearic acid were loaded into a three-neck flask. This mixture was then heated to 250°C under N₂ flow until it formed a yellow transparent solution. The solution was then cooled to room temperature and 4 g of trioctylphosphine oxide (TOPO) was added into the flask. The flask was then resealed and heated to 360°C under N₂ flow. A solution of 78mg Se, 0.4 g toluene, and 3.6 g trioctylphosphine (TOP) was then quickly injected into the reaction flask. The reaction solution temperature dropped to 285 °C after injection and then gradually increased to 300 °C over the course of approximately 1 minute. The 300°C growth temperature was then maintained for 1 minute and the heating mantle was then removed from the flask. The flask was cooled by natural convection to the ambient air until the temperature reached 150°C, at which point it was further cooled by immersion in a water bath. Once the temperature was below 50°C, the flask was removed from the Schlenk line and toluene was added to the reaction mixture to prevent solidification (1:1 toluene:reaction mixture). The CdSe nanocrystals were then precipitated by adding ethanol, and re-suspended in toluene two times. The CdSe nanocrystals were precipitated an additional time and re-suspended in hexane.

I.3. (N₂H₄)₂(N₂H₅)₂In₂Se₄ Precursor Synthesis

(N₂H₄)₂(N₂H₅)₂In₂Se₄ precursor was made by mixing 1.25mmol In₂Se₃, 3.75 mL of N₂H₄, and 1.25 mL of a 1 M solution of Se in N₂H₄. The mixture was stirred for two days and the resulting viscous light green solution was filtered with a 200 nm PVDF filter.

I.4. Ligand Exchange Process

In a typical ligand exchange process, two separate solutions were prepared: (A) CdSe nanocrystal solution in hexane (15 mg/mL) and (B) 0.25 M solution of (N₂H₄)₂(N₂H₅)₂In₂Se₄ in hydrazine. Solution B was then diluted with 2 mL of N₂H₄ and then 2 mL of Solution A was added to Solution B. This resulted in a bi-layer of liquid with the hexane phase on top and the N₂H₄ phase on bottom. This mixture was stirred for several hours, during which the hexane phase changed from dark to colorless and the hydrazine phase changed from colorless to dark, indicating that the ligand exchange was complete. The hexane was then removed and the hydrazine phase was filtered through a 200 nm PVDF filter. The CdSe nanocrystals with In₂Se₃ MCC ligands were then separated from unbound In₂Se₃ MCC precursor by precipitating via the addition of acetonitrile. The CdSe nanocrystals were then re-suspended in N₂H₄.

I.5. Nanocomposite Formation

100% In₂Se₃ nanocomposites were made by directly using the In₂Se₃ MCC precursor. ~100% CdSe nanocomposites were prepared with the solution of CdSe nanocrystals with In₂Se₃ MCC precursor ligands. Variation of CdSe mole fraction was achieved by mixing appropriate amounts of (N₂H₄)₂(N₂H₅)₂In₂Se₄ back into the solution of CdSe nanocrystals with In₂Se₃ MCC precursor ligands. Silicon substrates were prepared for nanocomposite deposition by cleaning with acetone, isopropanol, and UV ozone treatment. Nanocomposite thin film samples were prepared by spin-coating the solutions onto

the silicon substrates, drying for several minutes, and then heating to 350°C for 30 minutes. Film thickness was controlled by solution concentration and spin speed.

II. Materials Characterization

II.1. Thermogravimetric Analysis

Samples for thermogravimetric analysis (TGA) were prepared by drying the In_2Se_3 MCC precursor under a nitrogen flow to remove solvent. The dried precursor was orange in color and then crushed into a fine powder prior to the TGA measurement. TGA was done using a Mettler Toledo TGA/DSC1 Star system. The TGA measurement was done under a nitrogen atmosphere, during which the sample was heated at 2 °C/min from room temperature to 350 °C, maintained at 350 °C for 30 minutes, and then heated at 2 °C from 350 °C to 450 °C. The In_2Se_3 MCC precursor, $(\text{N}_2\text{H}_4)_2(\text{N}_2\text{H}_5)_2\text{In}_2\text{Se}_4$, contains weakly bound N_2H_4 groups that are easily removed during the abovementioned drying process. Consequently, a final decomposition product of In_2Se_3 implies a final mass between 69% and 76%. This corresponds to an initial condition between $(\text{N}_2\text{H}_4)_2(\text{N}_2\text{H}_5)_2\text{In}_2\text{Se}_4$ and $(\text{N}_2\text{H}_5)_2\text{In}_2\text{Se}_4$, respectively.

II.2. Transmission Electron Microscopy

Transmission electron microscope (TEM) images were taken by a Philips CM200-FEG high resolution TEM. TEM samples of the CdSe nanocrystals with organic ligands were prepared by drop-casting 50 μL of a dilute nanocrystal suspension onto a carbon film supported copper TEM grid. The nanocrystal diameter was determined with ImageJ by analyzing a representative TEM image containing 100 - 200 CdSe nanocrystals. In_2Se_3 TEM samples were prepared by drop casting 2 μL of a dilute $(\text{N}_2\text{H}_4)_2(\text{N}_2\text{H}_5)_2\text{In}_2\text{Se}_4$ precursor onto a Si_3Ni_4 window and then annealing at 350°C for 30 min. The grain size of In_2Se_3 was determined by manually measuring 60 grains and taking the average. The nanocomposite TEM samples were prepared in a similarly to the 100% In_2Se_3 samples.

II.3. Scanning Electron Microscopy

Scanning electron microscope (SEM) images were taken by a Nova 200 Nanolab SEM. SEM samples of nanocomposite were prepared by spin-coating the solution onto the silicon substrates, drying for several minutes, and then heating to 350°C for 30 minutes. The film thickness varied between 50 and 100 nm.

II.4. Elemental Composition Characterization

A 1.7 MV Tandem Ion Accelerator made by General Ionex was used for Rutherford backscattering spectroscopy (RBS) and particle-induced x-ray emission (PIXE). PIXE was done with 2.8 MeV H^+ ions and used to acquire the Cd:In ratio by analyzing the *K* x-ray emission. RBS was done with 2 MeV He^{2+} ions to acquire a Se peak and a combined Cd-In peak. The Cd:In ratio from PIXE along with the RBS data was then analyzed using an RBS fitting program (RUMP) to obtain the final elemental ratios. As mentioned in the main text, the ~100% CdSe composite samples had trace amounts of In due to the In_2Se_3 MCC surface functionalization of the CdSe nanocrystals. We note that this RBS-PIXE technique could not precisely determine the amount of trace In, but could confirm that the In was less than 3 at% of the composite.

II.5. X-ray Diffraction

Powder diffraction pattern was performed by a high-resolution X-ray diffractometer (XRD, PANALYTICAL X'PERT PRO) with $\text{CuK}\alpha$ X-ray source operating at 40 kV AND 40 mA. Thin film

XRD samples were prepared by spin coating solutions onto silicon substrates, and decomposing at 350°C for 30 minutes. Powder XRD samples were prepared similarly, but were drop cast instead of spin coated.

III. Calculation of Relative Peak Intensities for CdSe and CdIn₂Se₄

The peak intensity of an hkl reflection in a XRD pattern is proportional to:

$$I \propto |S|^2 \frac{M}{V_c}$$

where S is the structure factor, M is the multiplicity factor, and V_c is the unit cell volume. The structure factor can be calculated as:

$$S = \sum_i^N f_i \exp[-2\pi i(hx_i + ky_i + lz_i)]$$

where $(h k l)$ are the Miller indices of the plane of interest, $(x_i y_i z_i)$ are the position of the i th atom in the unit cell, N is the total number of atoms in the unit cell, and f is the atomic form factor. CdSe has a wurtzite structure with the following atomic positions:

Cd	(0 0 0)
Cd	(1/3 2/3 1/2)
Se	(0 0 3/8)
Se	(1/3 2/3 7/8)

CdIn₂Se₄ has a tetragonal structure with the following atomic positions:

Cd	(0 0 0)
In	(1/2 0 1/2)
In	(0 1/2 1/2)
Se	(1/4 1/4 1/4)
Se	(3/4 1/4 3/4)
Se	(1/4 3/4 3/4)
Se	(3/4 3/4 1/4)

The table below contains the parameters that were used for calculations of the relative peak intensities for CdSe and CdIn₂Se₄ as based on analysis of the structure factor, multiplicity factor, and unit cell volume. The intensity of the (1 1 1) peak in CdIn₂Se₄ is larger than the (0 0 2) and (1 0 0) peaks of CdSe by factors of 3.7 and 6.8, respectively (i.e. rightmost column of table below). Note that since these peaks all occur at approximately the same 2θ , the other factors contributing to XRD peak intensity (i.e. Lorentz factor, polarization factor, absorption factor, and temperature factor) should be approximately equivalent.

Peak	$ S ^2$	M	$V_c (\text{\AA}^3)$	$ S ^2 M / V_c (\text{\AA}^{-3})$
CdSe (1 0 0)	5.40×10^3	3	112	1.29
CdSe (0 0 2)	1.49×10^4	2	112	2.38
CdIn ₂ Se ₄ (1 1 1)	4.22×10^4	8	196	8.79

IV. Cahill-Pohl Model Calculation

The Cahill-Pohl model (note that the Cahill-Pohl model is also commonly referred to as the “minimum thermal conductivity model” and the “amorphous limit”) is a simple calculation that is commonly used to estimate the thermal conductivity of amorphous materials. It is given by the equation:²

$$k_{min} = \left(\frac{\pi}{6}\right)^{1/3} k_B n^{2/3} \sum_i v_i \left(\frac{T}{\Theta_i}\right)^2 \int_0^{\Theta_i/T} \frac{x^3 e^x}{(e^x - 1)^2} dx$$

where k_B is the Boltzmann constant, n is the number density of atoms, T is the absolute temperature, and v_i and Θ_i are the speed of sound and Debye temperature of the i th phonon branch. In our implementation of the Cahill-Pohl model, we used the following properties for wurtzite phase CdSe:³

n	$3.66 \times 10^{28} \text{ m}^{-3}$
$v_{\text{longitudinal}}$	3780 m/s
$v_{\text{transverse},1}$	1490 m/s
$v_{\text{transverse},2}$	1490 m/s

The values for the Debye temperatures can be calculated as:⁴

$$\Theta_i = v_i \left(\frac{\hbar}{k_B}\right) (6\pi^2 n)^{1/3}$$

where \hbar is the reduced Planck constant. Although there is no available literature on the speed of sound for $\gamma\text{-In}_2\text{Se}_3$, there is available literature for $\alpha\text{-In}_2\text{Se}_3$.⁵ Since an amorphous material should be phase independent, we use the properties of $\alpha\text{-In}_2\text{Se}_3$ in our calculations for the Cahill-Pohl model. Furthermore, since our thermal conductivity measurements of $\gamma\text{-In}_2\text{Se}_3$ were approximately along the c-axis, we use the c-axis properties of $\alpha\text{-In}_2\text{Se}_3$ for our calculation:

n	$7.29 \times 10^{27} \text{ m}^{-3}$
$v_{\text{longitudinal}}$	2679 m/s
$v_{\text{transverse},1}$	1728 m/s
$v_{\text{transverse},2}$	1728 m/s

Using the above equations and values, we estimate that the thermal conductivities of amorphous CdSe and amorphous In_2Se_3 are 0.40 W/m-K and 0.13 W/m-K, respectively.

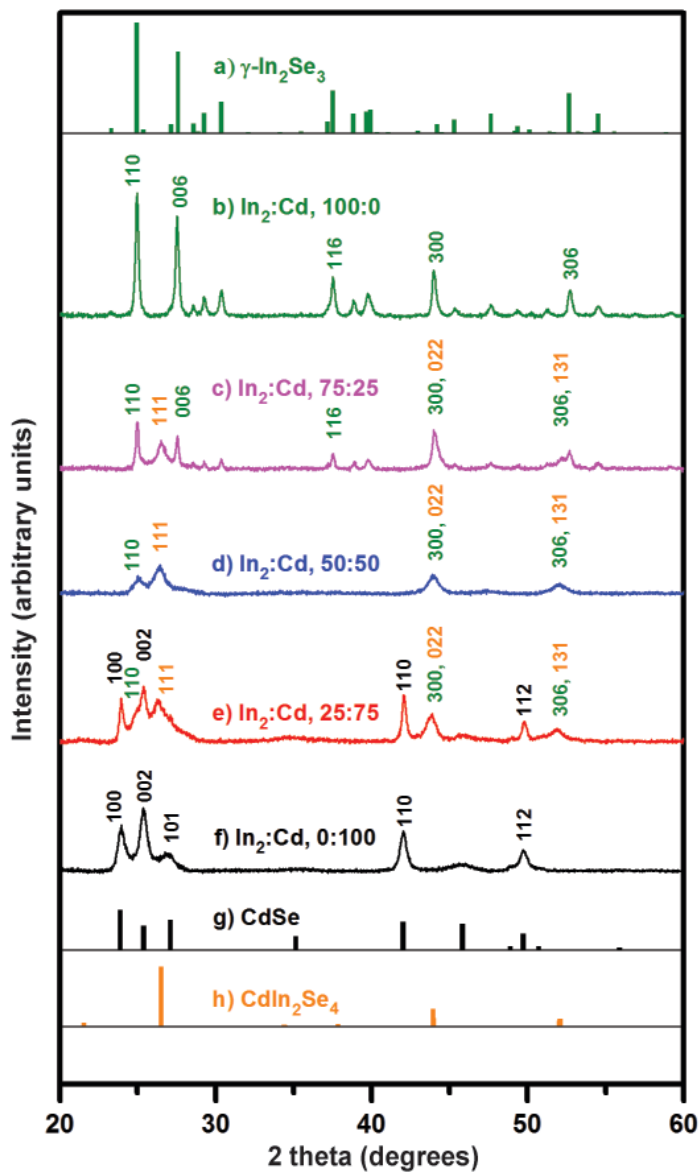


Figure S1. X-ray diffraction patterns of (a) γ - In_2Se_3 powder diffraction file 01-089-0658, nanocomposite powders with In_2 :Cd ratios of (b) 100:0, (c) 75:25, (d) 50:50, and (e) 25:75, (f) 0:100, (g) CdSe powder diffraction file 01-077-0021, and (h) CdIn_2Se_4 powder diffraction file 00-056-1124.

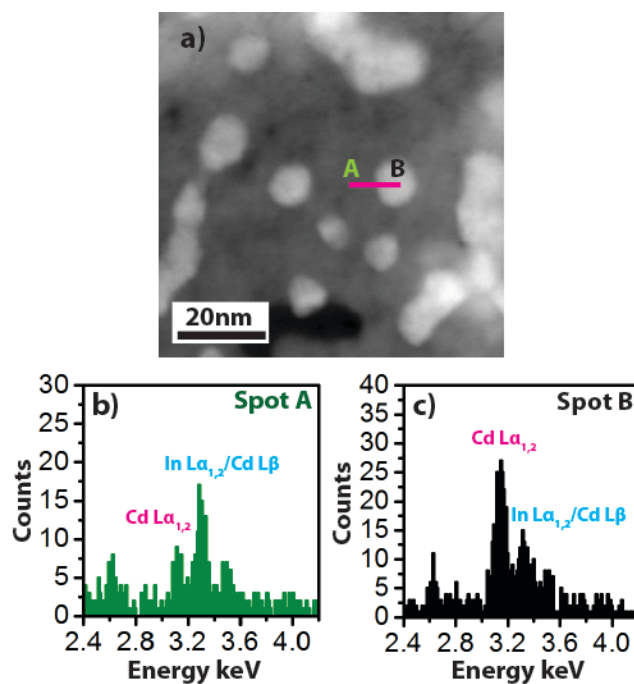


Figure S2. (a) Dark field scanning transmission electron microscopy image of nanocomposite with In_2 :Cd ratio of 50:50. (b) Energy-dispersive X-ray spectroscopy (EDX) on Spot A, which corresponds to the In_2Se_3 matrix (c) EDX on Spot B, which corresponds to a CdSe nanoparticle. The EDX peak at ~ 3.1 keV corresponds to $L_{\alpha 1,2}$ transitions of Cd whereas the peak at ~ 3.3 keV corresponds to both the L_{β} transitions of Cd and the $L_{\alpha 1,2}$ transitions of In. Since the ratio of the $L_{\alpha 1,2}$ to L_{β} transition in Cd is 1.9,⁶ it can be seen that Spot A is In-rich whereas Spot B is Cd-rich. Given the nanoscale features of our composite and since x-rays are generated from a relatively large volume during EDX, our apparent detection of Cd in the In_2Se_3 matrix and vice versa is to be expected.

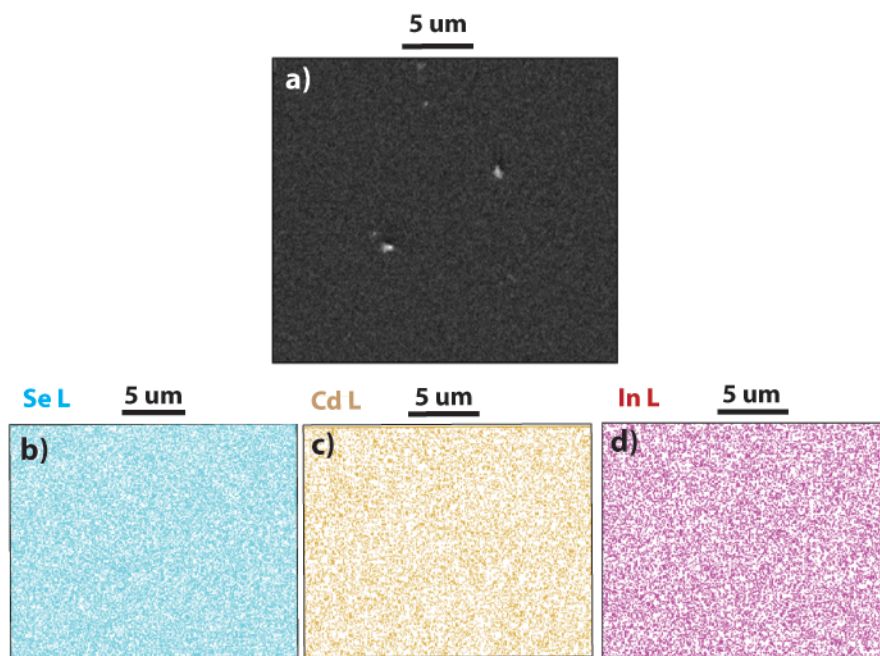


Figure S3. a) Scanning electron microscopy image of a nanocomposite with In_2Cd ratio of 41:59. Energy-dispersive X-ray (EDX) maps of (b) Se, (c) Cd, and (d) In show an uniform elemental distribution in the composite.

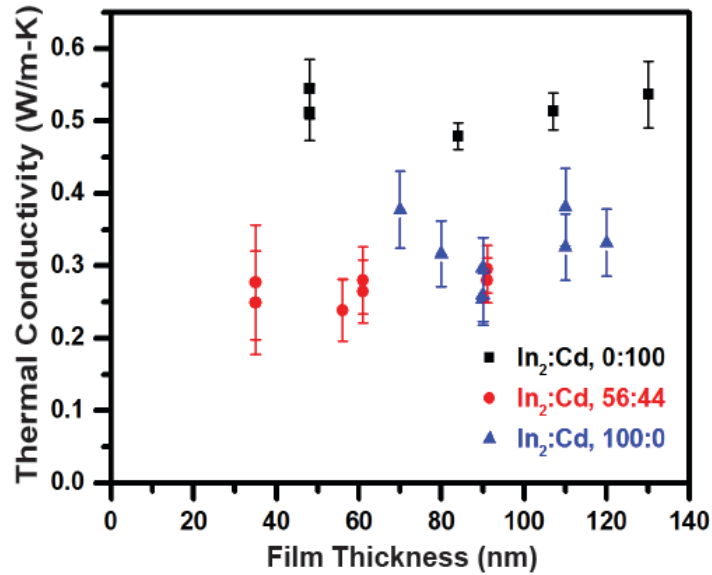


Figure S4. Thermal conductivity of nanocomposite thin films as a function of film thickness for composites with In₂:Cd ratios of 0:100 (black squares), 56:44 (red squares), and 100:0 (blue triangles). The lack of correlation between thermal conductivity and film thickness indicates that transport in these films is diffusive and that the thermal contact resistances between layers of the 3 ω thermal conductivity samples are negligible.

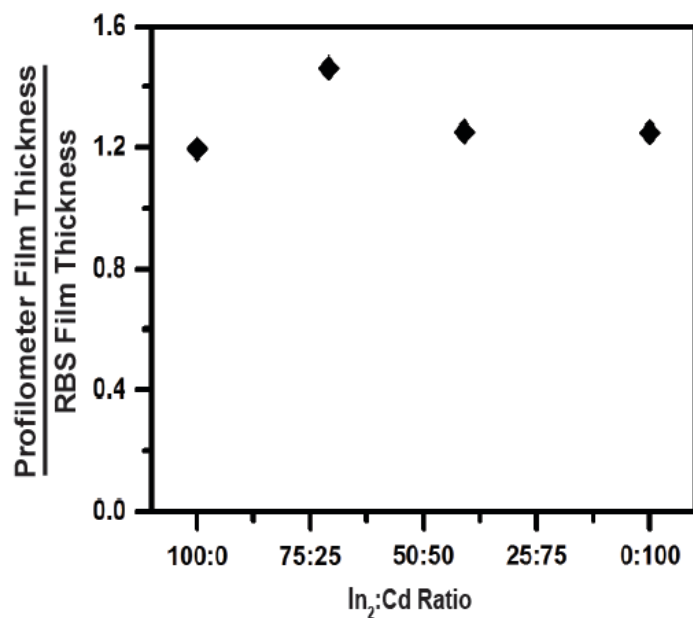


Figure S5. Ratio of film thickness measured by profilometry to film thickness measured by Rutherford backscattering spectroscopy (RBS) for composites with varying In₂:Cd ratios. Film thicknesses determined by Rutherford backscattering spectroscopy used the measured areal atomic density and assumed fully dense films. All samples in this figure had film thicknesses of approximately 50 – 60 nm.

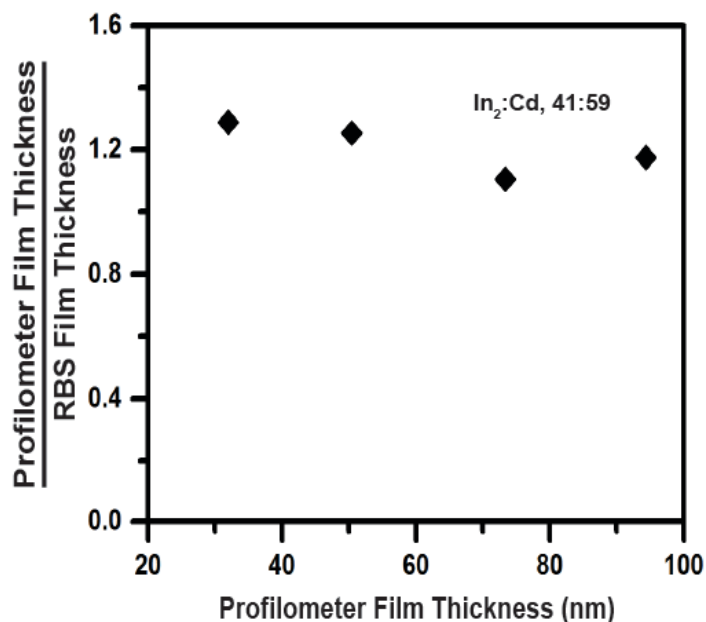


Figure S6. Ratio of film thickness measured by profilometry to film thickness measured by Rutherford backscattering spectroscopy (RBS) for composites with varying thicknesses. Film thicknesses determined by Rutherford backscattering spectroscopy used the measured areal atomic density and assumed fully dense films. All samples in this figure have an In₂:Cd ratio of 41:59.

References

1. Qu, L. H. P., Z.A; Peng,X.G.; *Nano Lett.* 2001, **1**, 333-337.
2. Cahill, D. G.; Watson, S. K.; Pohl, R. O. *Phys. Rev. B* 1992, **46**, 6131-6140.
3. Mohr, M.; Thomsen, C. *Nanotechnology* 2009, **20**, 115707.
4. Kittel, C., *Introduction to Solid State Physics*. 7th ed.; John Wiley and Sons, Inc.: 1996.
5. Raranskii, N. D.; Balazyuk, V. N.; Kovalyuk, Z. D.; Mel'nik, N. I.; Gevik, V. B. *Inorg. Mater.* 2011, **47**, 1174-1177.
6. Thompson, A. C., *X-Ray Data Booklet*. Los Angeles 2009.